

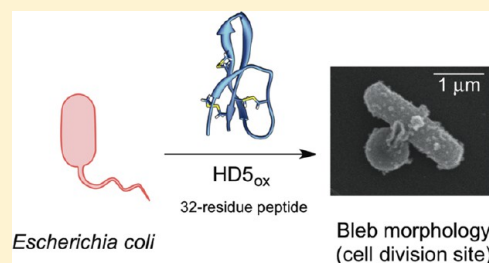
Visualizing Attack of *Escherichia coli* by the Antimicrobial Peptide Human Defensin 5

Haritha R. Chileveru, Shion A. Lim, Phoom Chairatana, Andrew J. Wommack, I-Ling Chiang, and Elizabeth M. Nolan*

Department of Chemistry, Massachusetts Institute of Technology, Cambridge, Massachusetts 02139, United States

Supporting Information

ABSTRACT: Human α -defensin 5 (HD5) is a 32-residue cysteine-rich host-defense peptide that exhibits broad-spectrum antimicrobial activity and contributes to innate immunity in the human gut and other organ systems. Despite many years of investigation, its antimicrobial mechanism of action remains unclear. In this work, we report that HD5_{ox}, the oxidized form of this peptide that exhibits three regiospecific disulfide bonds, causes distinct morphological changes to *Escherichia coli* and other Gram-negative microbes. These morphologies include bleb formation, cellular elongation, and clumping. The blebs are up to $\sim 1\ \mu\text{m}$ wide and typically form at the site of cell division or cell poles. Studies with *E. coli* expressing cytoplasmic GFP reveal that HD5_{ox} treatment causes GFP emission to localize in the bleb. To probe the cellular uptake of HD5_{ox} and subsequent localization, we describe the design and characterization of a fluorophore–HD5 conjugate family. By employing these peptides, we demonstrate that fluorophore–HD5_{ox} conjugates harboring the rhodamine and coumarin fluorophores enter the *E. coli* cytoplasm. On the basis of the fluorescence profiles, each of these fluorophore–HD5_{ox} conjugates localizes to the site of cell division and cell poles. These studies support the notion that HD5_{ox}, at least in part, exerts its antibacterial activity against *E. coli* and other Gram-negative microbes in the cytoplasm.



Bacterial infections and the considerable rise in antibiotic resistance in hospital and community settings pose significant problems for global health initiatives.^{1,2} The dearth of new antibiotics in the drug pipeline as well as an incomplete comprehension of human innate immunity and microbial pathogenesis further confound efforts to address these challenges.^{3,4} Bacterial pathogens must overcome the innate immune system, which provides first-line defense against microbial invaders, to cause human disease. Fundamental investigations that address the molecular interworkings of the innate immune system are critical for improving our understanding of the host–microbe interaction and allowing the development of new therapeutic strategies for infectious disease. Antimicrobial peptides (AMPs) and/or host-defense peptides are important components of the innate immune system.^{5–8} In humans, defensins^{7,9} and the cathelicidin LL-37^{10,11} are abundant host-defense peptides expressed and utilized by neutrophils and epithelial cells of the gastrointestinal tract, urogenital tract, airway, and skin.¹² Mammalian defensins are cysteine-rich peptides that are classified as α -, β -, and θ -defensins on the basis of regiospecific disulfide linkage patterns.¹² α -Defensins exhibit three disulfide bonds in the oxidized forms with Cys^I–Cys^{VI}, Cys^{II}–Cys^{IV}, and Cys^{III}–Cys^V linkages and have three-stranded β -sheet structures.⁷ In humans, six α -defensins are known.⁷ The enteric α -defensin HD5 (Figure 1), the focus of this work, is an abundant constituent of small intestinal Paneth cell granules.^{13–16} Although human defensins are established contributors to

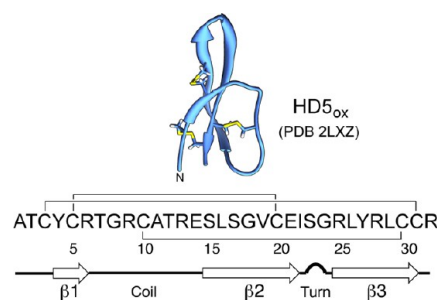


Figure 1. Structure of the HD5_{ox} monomer determined by solution NMR (PDB entry 2LXZ)¹⁹ and amino acid sequence. The regiospecific disulfide bond linkages and secondary structure are indicated.

immunity, and many exhibit broad-spectrum *in vitro* antimicrobial activity, details pertaining to the physiological function of each peptide are often unclear.^{12,17,18} In this work, we focus on the fundamental and outstanding question of how HD5 kills bacteria.

How defensins kill bacteria as well as how *in vitro* antibacterial activity relates to the physiological milieu are questions of current interest and debate.¹⁷ The oxidized α -defensins display remarkable similarity in their tertiary

Received: December 3, 2014

Revised: February 7, 2015

Published: February 9, 2015

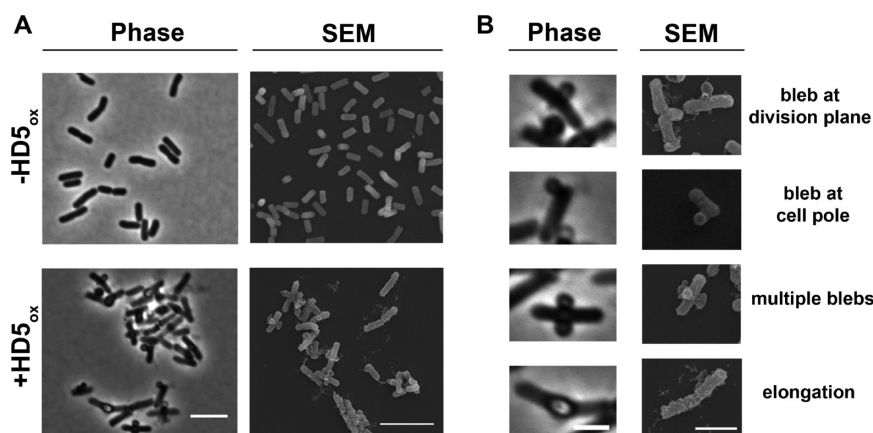


Figure 2. HD5_{ox} causes distinct morphological changes in *E. coli* that include bleb formation, cellular elongation, and clumping. (A) Phase-contrast and SEM images of *E. coli* ATCC 25922 (1×10^8 CFU/mL) in the absence (–HD5_{ox}) or presence (+HD5_{ox}) of 20 μ M HD5_{ox} (scale bar of 5 μ m). (B) Phase-contrast and SEM images of single cells illustrate the various morphologies caused by HD5_{ox} (scale bar of 2 μ m).

structure, and most characterized to date are cationic and amphipathic.²⁰ Moreover, defensins from various organisms have the capacity to disrupt bacterial cell membranes.^{21–23} On the basis of early investigations, including seminal structural studies of HNP3,²⁴ a working model whereby defensins kill bacteria by nonspecific membrane destabilization was presented.^{21,24} Over the years, this type of model was generalized for many defensins and other antimicrobial peptides.¹⁷ Nevertheless, defensins exhibit remarkable diversity in primary sequence, and recent studies support alternative mechanisms of action for some family members. Fungal plectasin,²⁵ oyster defensin,²⁶ and fungal copisin²⁷ bind lipid II and block cell wall biosynthesis. The human defensins human neutrophil peptide 1 (HNP1, α -defensin)²⁸ and human β -defensin 3 (HBD3)²⁹ are also reported to bind lipid II to varying degrees.³⁰ Studies of HBD3 attributed the *in vitro* antibacterial activity against *Staphylococcus aureus* to lipid II binding and subsequent cell wall lysis.²⁹ Recently, human β -defensin 2 (HBD2) was found to localize at septal foci of *Enterococcus faecalis* and disrupt virulence factor assembly.³¹ Human α -defensin 6 (HD6) lacks antimicrobial activity *in vitro* and is proposed to serve a host-defense function by self-assembling into a weblike structure termed a “nanonet” that captures bacteria in the intestinal lumen.^{32,33} Taken together, these investigations highlight tremendous variation in defensin mechanism of action despite similar tertiary structures and demonstrate that membrane permeabilization is only one of the many factors that contribute to the *in vitro* antimicrobial activities demonstrated by this vast peptide family.

Our laboratory has initiated a research program focused on understanding the biophysical properties and biological functions of human defensins that are produced and released in the small intestine. Paneth cells,¹⁶ located in the crypts of Lieberkühn, contain granules that store two α -defensins, HD5 and HD6, as well as other antimicrobial peptides, proteases, and a labile zinc pool of unknown function.^{34,35} HD5 is the most abundant Paneth cell antimicrobial peptide,³⁶ and it exhibits broad-spectrum antimicrobial activity *in vitro*.^{37–40} Moreover, transgenic mice expressing HD5 are more resistant to *Salmonella* challenge than wild-type mice,⁴¹ and studies of the resident intestinal microbiota suggest that HD5 contributes to controlling its composition.^{41,42} In humans suffering from ileal Crohn’s disease, an inflammatory disorder of the small bowel, a deficiency in Paneth cell defensins has been reported.³⁶ Despite

these compelling observations from animal models and clinical studies, the antimicrobial mechanism of action of HD5 is not well understood.

HD5 is a 32-residue peptide with an overall charge of +4 at neutral pH (Figure 1). Over the past decade, structure–activity relationship studies of HD5_{ox} evaluated how quaternary structure,^{40,43} disulfide linkages,^{44,45} cationic residues,⁴⁶ the canonical α -defensin salt bridge between [Arg⁶] and [Glu¹⁴],⁴⁷ and chirality⁴⁸ contribute to its *in vitro* bactericidal activity. Results from several recent studies probing interactions between HD5_{ox} and *Escherichia coli* support a model whereby (i) the Gram-negative outer membrane serves as a permeability barrier for HD5_{ox}^{49,50} and (ii) the inner membrane becomes damaged as a result of HD5_{ox} exposure.⁴⁴

In this work, we utilize microscopy to investigate the attack of HD5_{ox} on Gram-negative bacteria. We establish that *E. coli* cells treated with native HD5_{ox} exhibit distinct morphologies that include clumping, cell elongation, and formation of one or more cellular blebs typically at the cell poles or division site. We demonstrate that similar morphological changes occur for other Gram-negative bacteria, including the opportunistic human pathogens *Acinetobacter baumannii* and *Pseudomonas aeruginosa*, following HD5_{ox} exposure. Through the design, characterization, and utilization of a fluorophore–HD5 conjugate family, we report that rhodamine- and coumarin-modified HD5_{ox} enter the *E. coli* cytoplasm. Moreover, these fluorophore–HD5_{ox} conjugates preferentially localize at cell poles and cell division sites in *E. coli*, suggesting locales of a possible intracellular target.

RESULTS AND DISCUSSION

HD5 Causes Distinct Morphological Changes in *E. coli*.

For morphology studies, we chose to image Gram-negative *E. coli*. This organism is a commensal microbe of the human gut as well as a pathogen of the gut and urogenital tract, and a number of studies have probed the antibacterial activity of HD5_{ox} against this strain.^{37,44,47} In antimicrobial activity (AMA) assays, the concentration of HD5_{ox} required to kill *E. coli* (e.g., lethal dose 99.99% or 4-fold log reduction in colony-forming units per milliliter) depends on the number of colony-forming units (CFU). Our standard AMA assay for evaluating HD5_{ox} activity employs mid log-phase bacteria at $\approx 1 \times 10^6$ CFU/mL cultured in an AMA buffer [10 mM sodium phosphate buffer (pH 7.4) and 1% (v/v) TSB without

dextrose]. Under these conditions, the concentration of HD₅_{ox} required to kill 99.99% of *E. coli* is $\approx 4 \mu\text{M}$ depending on the precise starting number of colony-forming units per milliliter. Treatment of mid log-phase *E. coli* ATCC 25922 (1×10^6 CFU/mL) with HD₅_{ox} (2 and 4 μM) under standard AMA assay conditions resulted in marked changes to the bacterial morphology that could be observed by phase-contrast microscopy. The morphological changes included the formation of large bulges, hereafter called blebs (Figure S1 of the Supporting Information). To facilitate the visualization of more cells per experiment, we modified the standard AMA conditions and employed a greater number of cells (1×10^8 CFU/mL) and higher concentrations of HD₅_{ox} (0–80 μM). Under these conditions, HD₅_{ox} displays AMA, and an ≈ 2 -fold log reduction in the number of CFU/mL is observed following treatment of the *E. coli* with 40 μM HD₅_{ox} (Figure S2 of the Supporting Information). Moreover, the *E. coli* displayed distinct morphological changes as observed in the preliminary experiment (Figure S1 of the Supporting Information). On the basis of this similarity, we employed the modified conditions with greater cell density and higher HD₅_{ox} concentration for further imaging experiments. The morphologies observed under these conditions included cellular elongation and the formation of blebs (Figure 2). Clumping of *E. coli* was also observed. Bacterial cells with lengths of $\geq 5 \mu\text{m}$ were categorized as elongated, and cells with lengths in the 10–15 μm range were periodically observed following HD₅_{ox} treatment. The blebs were typically localized at the cell division sites and cell poles; however, some bacteria displayed blebs along the cell body, and some bacteria exhibited multiple blebs per cell. The blebs remained intact during the centrifugation and wash steps required for scanning electron microscopy (SEM) sample preparation. Indeed, the blebs as well as what appeared to be outer membrane vesicles (Figure S3 of the Supporting Information) and cellular debris (*vide infra*) were markedly apparent in SEM images (Figure 2).

Neither blebs nor elongation was observed for untreated cells, and the number of cells exhibiting these morphological changes increased with an increasing HD₅_{ox} concentration (0–80 μM) (Figure 3). Following exposure to 20 μM HD₅_{ox},

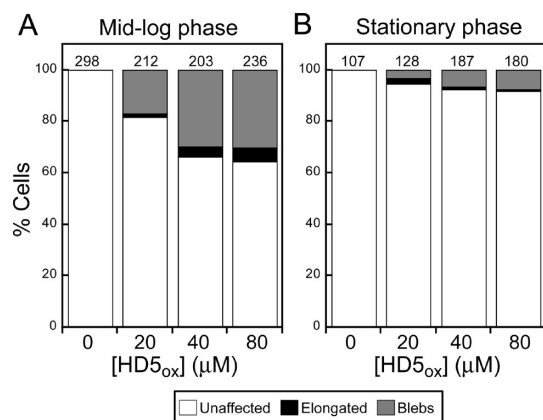


Figure 3. Effect of HD₅_{ox} treatment on *E. coli* ATCC 25922 morphology. The cells (1×10^8 CFU/mL) were treated with varying concentrations of HD₅_{ox} for 1 h at 37 °C [10 mM sodium phosphate buffer (pH 7.4) and 1% (v/v) TSB]. (A) Quantification of unaffected as well as elongated and bleb morphologies for mid log-phase *E. coli*. (B) Quantification for stationary-phase *E. coli*. The number above each bar indicates the number of cells counted.

$\approx 17\%$ of cells exhibited blebs and 2% were elongated ($n = 212$ cells). These values increased to $\approx 30\%$ and $\geq 4\%$, respectively, at $\geq 40 \mu\text{M}$ HD₅_{ox} ($n = 203$ cells). We performed time-course experiments in which *E. coli* cells were exposed to 20 μM HD₅_{ox} on the microscope stage and imaged over time (≈ 2 h). Many of the treated cells displayed blebs, and the blebbing cells did not lyse over the course of this experiment (Figure S4 of the Supporting Information). Propidium iodide (PI) uptake was therefore employed to evaluate the viability of HD₅_{ox}-treated cells. The cells exhibiting blebs were labeled with PI, which indicated that bleb formation correlated with cell death (Figure S5 of the Supporting Information). The morphological changes observed for *E. coli* ATCC 25922 were comparable to those we recently reported for *E. coli* K-12 and select mutants from the Keio Collection.⁵⁰

The susceptibility of *E. coli* to HD₅_{ox} depends on the growth phase, and stationary-phase cultures exhibit resistance to HD₅_{ox} relative to mid log-phase cultures as observed for other defensins.²¹ Under the standard AMA assay conditions employed in this work, treatment of mid log-phase *E. coli* with 4 μM HD₅_{ox} resulted in an ≈ 4 -fold log reduction in the number of colony-forming units per milliliter, whereas only an ≈ 2 -fold log reduction was observed for stationary-phase *E. coli* (Figure S6 of the Supporting Information). In agreement with this trend, fewer morphological changes were observed for stationary-phase cells treated with HD₅_{ox} (Figure 3 and Figure S6 of the Supporting Information). Taken together, the microscopy and AMA assays with HD₅_{ox} and *E. coli* provided a correlation between bacterial susceptibility and altered cellular morphology.

Treatment of *E. coli* with Other AMPs Does Not Result in the Bleb Morphology.

We questioned whether other antimicrobial peptides confer the same morphological changes observed for HD₅_{ox} under the experimental conditions used in this work. Prior biophysical studies proposed the ability of the murine Paneth cell defensin cryptdin-4 to induce negative curvature on bacterial membranes, resulting in structures called blebs or pores.⁵¹ To visualize the effect of cryptdin-4 on *E. coli* morphology, we first obtained cryptdin-4 by overexpression in *E. coli* and confirmed its antimicrobial activity (Figure S9 of the Supporting Information). The *E. coli* treated with cryptdin-4 (20 μM) did not form large blebs as observed with HD₅_{ox} (Figure 4). Likewise, *E. coli* did not exhibit blebs following exposure to the pore-forming antimicrobial peptide melittin⁵² (20 μM), the LPS-associated membrane-destabilizing peptide colistin⁵³ (20 μM), or the pore-forming antimicrobial peptide human LL-37⁵⁴ (20 μM) (Figure 4). The bacteria treated with LL-37 were somewhat elongated relative to the untreated control cells. Small membrane protrusions (<100 nm wide) and surface roughness observed for bacteria treated with AMPs such as magainin 2⁵⁵ and Bac8c⁵⁶ have been described as blebs. To the best of our knowledge, larger blebs ($\sim 1 \mu\text{m}$ wide), formed preferentially at poles and cell division sites as observed for HD₅_{ox} have not been reported for a human host-defense peptide. The most similar bleb morphologies we identified in the literature are the bulges that result from β -lactam treatment.⁵⁷ Moreover, a knockout mutant of *elyC*,⁵⁸ an inner membrane protein involved in peptidoglycan synthesis from the Keio Collection, and some Tol-Pal mutants of *Caulobacter crescentus*⁵⁹ are reported to display large blebs.

On the basis of this modest AMP screen, we concluded that HD₅_{ox} affects *E. coli* differently compared to the other AMPs considered in this work, including the murine α -defensin

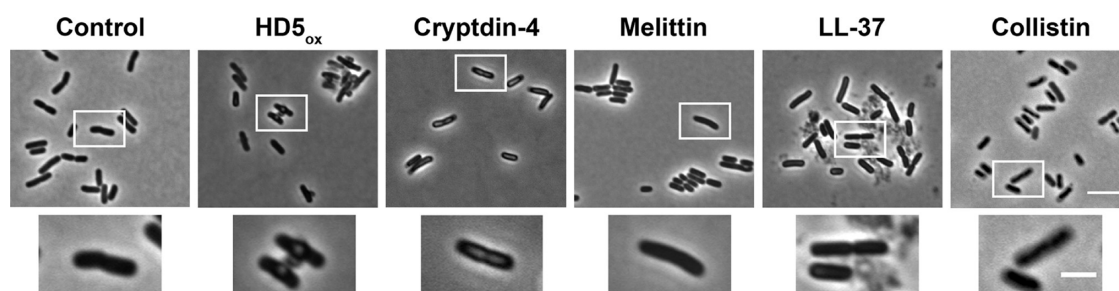


Figure 4. Consequences of various antimicrobial peptides on *E. coli* morphology. *E. coli* ATCC 29522 (1×10^8 CFU/mL, mid log phase) were exposed to each peptide (20 μ M) for 1 h at 37 °C [10 mM sodium phosphate buffer (pH 7.4) and 1% (v/v) TSB] prior to imaging. In the top panels, the scale bar is 5 μ m; in the bottom panels, the scale is 2 μ m.

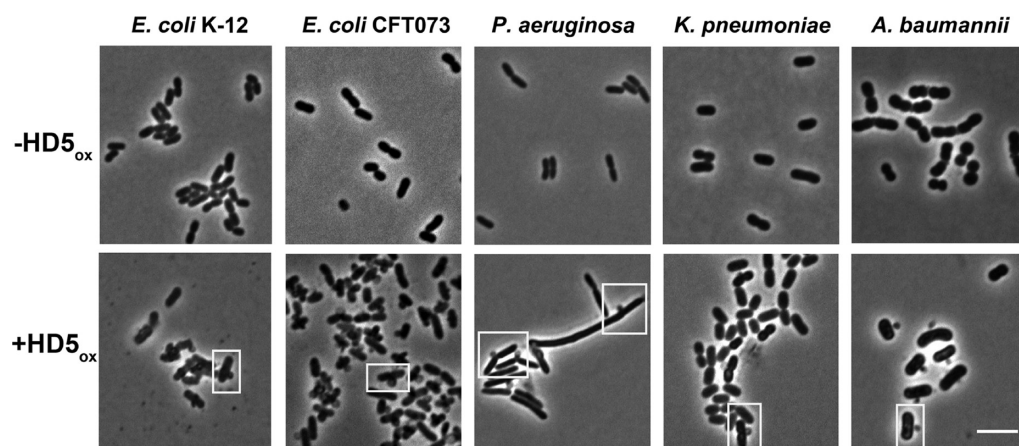


Figure 5. Effect of HD5_{ox} exposure on the morphology of Gram-negative bacteria. Each microbe (1×10^8 CFU/mL, mid log phase) was exposed to HD5_{ox} (20 μ M except for *P. aeruginosa*, for which 40 μ M was used) for 1 h at 37 °C [10 mM sodium phosphate buffer (pH 7.4) and 1% (v/v) TSB] prior to imaging. The scale bar is 5 μ m. Additional images are provided in Figure S8 of the Supporting Information.

cryptdin-4. Although morphology comparisons alone do not provide detailed insight into antibacterial mechanisms, our imaging results suggest that the mechanism of action of HD5_{ox} against *E. coli* cannot be explained fully by membrane permeabilization.

HD5_{ox} Causes Similar Morphological Changes in Other Gram-Negative Organisms. HD5_{ox} exhibits broad-spectrum antibacterial activity,^{37,38,40} and the question of whether its mechanism of action is general or strain-specific remains unclear. Several structure–activity relationship studies indicated that HD5_{ox} operates by different mechanisms for Gram-negative and -positive organisms, but these studies were limited to comparisons between *E. coli* and *S. aureus*.^{44,45,48} To delineate whether HD5_{ox} perturbs the morphologies of other Gram-negative strains, four human pathogens, *A. baumannii* 17978, *Klebsiella pneumoniae* 13883, *P. aeruginosa* PAO1, and *E. coli* CFT073, were evaluated along with the laboratory strain *E. coli* K-12 (Figure 5). Similar to nonpathogenic *E. coli* ATCC 25922 and K-12, bleb formation, elongation, and clumping were observed for the pathogenic strains. We previously reported that *A. baumannii* exhibits a relatively high sensitivity to HD5_{ox}.⁴⁰ In accordance with this observation, *A. baumannii* displayed blebs at 10 μ M HD5_{ox} (Figure S8 of the Supporting Information). *P. aeruginosa* is less susceptible to HD5_{ox} killing,⁴⁰ and relatively high concentrations (40 μ M) of HD5_{ox} were required to elicit bleb formation for this strain (Figure S8 of the Supporting Information).

Morphological Changes Are Attenuated by Salt and Divalent Metal Ions. The *in vitro* antimicrobial activity of

many defensins is attenuated by the presence of salt and divalent cations.⁶⁰ This phenomenon is commonly attributed to a disruption of electrostatic interactions between the cationic defensin and anionic bacterial cell membrane.¹⁷ Like many defensins, the antibacterial activity of HD5_{ox} is attenuated by millimolar concentrations of sodium chloride.³⁸ We observed that NaCl prevents bleb formation and other morphological changes associated with HD5_{ox} activity. Indeed, *E. coli* cotreated with HD5_{ox} (40 μ M) and NaCl (200 mM) displayed a smooth morphology similar to that of the untreated control (Figure S7 of the Supporting Information). The divalent cations Ca(II), Mg(II), and Zn(II) also blocked HD5_{ox} activity (Figure S7 of the Supporting Information). This effect was most potent for Zn(II), for which a 2:1 Zn(II):HD5_{ox} molar ratio resulted in a loss of antibacterial activity and HD5_{ox}-associated morphologies. This observation is of broad interest because the Paneth cell granules, which harbor HD5, also contain a labile zinc pool of unknown function.³⁴

Disulfide Bonds Are Necessary for the Bleb Morphology. The canonical α -defensin disulfide array provides a three-stranded β -sheet fold to each HD5_{ox} monomer. This compact structure orients the positively charged residues on one face of the peptide and the hydrophobic residues on the opposite, rendering HD5 amphipathic.¹⁹ To investigate the structural requirements for HD5_{ox} activity, we evaluated the consequences of treating *E. coli* with three HD5 derivatives, HD5-TE, HD5-CD, and HD5[E21S]_{ox}, selected to probe the disulfide array as well as quaternary structure. HD5-TE is a linear disulfide-null analogue where the six cysteines are carbox-

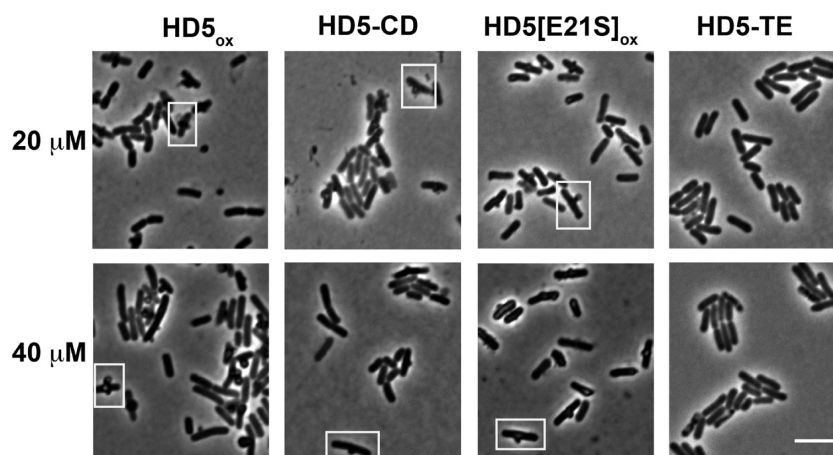


Figure 6. *E. coli* morphologies in the presence of HD5 derivatives reveal that the disulfide bonds are necessary for bleb formation. *E. coli* ATCC 25922 (1×10^8 CFU/mL, mid log phase) was exposed to each peptide for 1 h at 37 °C [10 mM sodium phosphate buffer (pH 7.4) and 1% (v/v) TSB] prior to imaging. The scale bar is 5 μ m.

ymethylated with 2-iodoacetamide.⁶¹ Defensins have the propensity to self-associate, and in prior work, we reported that HD5_{ox} forms tetramers at neutral pH.¹⁹ HD5-CD is a C₂-symmetric covalent dimer of HD5_{ox} with a cationic surface that results from intermolecular disulfide exchange between the Cys⁵–Cys²⁰ disulfide bonds (canonical Cys^{II}–Cys^{IV}) of two HD5 monomers.⁴⁰ We also prepared and characterized HD5[E21S]_{ox}, a new HD5_{ox} mutant that forms a noncovalent dimer, but not a tetramer, at neutral pH (Table S3 and Figure S23 of the Supporting Information).

E. coli cells treated with HD5-CD or HD5[E21S]_{ox} were indistinguishable from those treated with HD5_{ox} (Figure 6), in agreement with antimicrobial activity assays in which both HD5[E21S]_{ox} and HD5-CD killed *E. coli* (Figure S10 of the Supporting Information). In contrast, the antimicrobial activity of linear and unstructured HD5-TE against *E. coli* was attenuated (2-fold log reduction in the CFU/mL at 16 μ M) relative to HD5_{ox}. HD5-TE did not cause bleb formation (Figure 6); however, SEM revealed that the cells treated with HD5-TE were corrugated and frequently elongated (Figure S11 of the Supporting Information). These results highlight the importance of cysteine residues housed in disulfide linkages in the overall antimicrobial activity of HD5 and the induced morphological changes.

Cytoplasmic GFP is Observed in the Blebs. The blebs observed in this work are reminiscent of the cellular morphologies that result from treatment of *E. coli* with β -lactams, and *E. coli* strains expressing GFP have proven to be useful in imaging studies of β -lactam action.^{57,62} Guided by this work, we investigated the contents as well as time-dependent formation of the blebs by employing an *E. coli* strain that expresses cytoplasmic GFP (*E. coli* cyto-GFP). Mid log-phase *E. coli* cyto-GFP formed blebs following exposure to HD5_{ox}. The blebs displayed GFP emission, and the GFP emission from the cell body was markedly reduced, suggesting that cytoplasmic contents localized to the blebs (Figure 7). Some additional phenotypes were observed for dividing cells. In several instances in which a dividing cell exhibited a bleb at the cell division site, the GFP localization differed between the daughter cells (Figure S12 of the Supporting Information). Moreover, for cells with blebs at the cell division site, the GFP intensity in the region between the two daughter cells was relatively weak, indicating the presence of a membrane at the

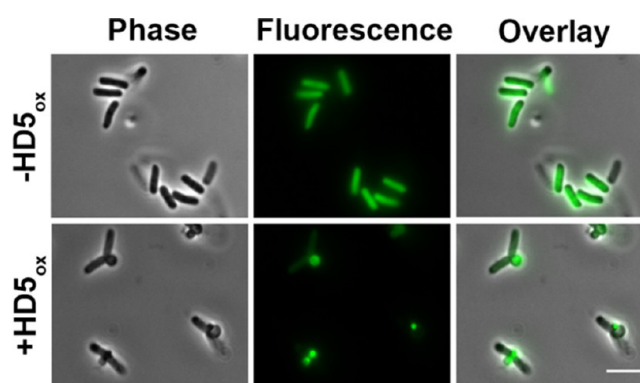


Figure 7. Treatment of *E. coli* cyto-GFP with HD5_{ox} reveals that the cytoplasmic contents leak into the blebs. *E. coli* cyto-GFP (1×10^7 CFU/mL, mid log phase) were exposed to 4 μ M HD5_{ox} for 1 h at 37 °C [10 mM sodium phosphate buffer (pH 7.4) and 1% (v/v) TSB] prior to imaging. The scale bar is 5 μ m.

division plane. In agreement with this observation, labeling HD5_{ox}-treated *E. coli* ATCC 25922 with the membrane-binding dye FM4-64 confirmed the presence of this membrane (Figure S13 of the Supporting Information).

Cell viability, as observed by PI uptake, was inversely correlated to the overall GFP fluorescence intensity of the bacteria (Figure S14 of the Supporting Information). When *E. coli* cyto-GFP cells (1×10^8 CFU/mL) were treated with HD5_{ox} (20 μ M) and subsequently stained as a result of PI uptake (5 μ g/mL), the cells with brighter GFP emission and fewer morphological defects exhibited less PI labeling than cells that were affected by HD5_{ox}.

In agreement with studies using *E. coli* ATCC 25922 (Figure 3), negligible changes in morphology and GFP localization were observed for HD5_{ox}-treated *E. coli* cyto-GFP in the stationary phase. To obtain quantitative comparisons, the GFP intensity and morphological changes for both mid log-phase and stationary-phase *E. coli* cyto-GFP were analyzed (Figure S15 of the Supporting Information). The mean cell length for the mid log-phase cells increased from 2.8 ± 0.8 to 3.4 ± 1.0 μ m (Student's *t* test, *t* value = 6.32, *t* probability < 0.0001) with an increasing HD5_{ox} concentration (0–80 μ M), and the mean GFP fluorescence intensity decreased accordingly (from 155 ± 48 to 93 ± 47 units). Only minor changes in both cell lengths

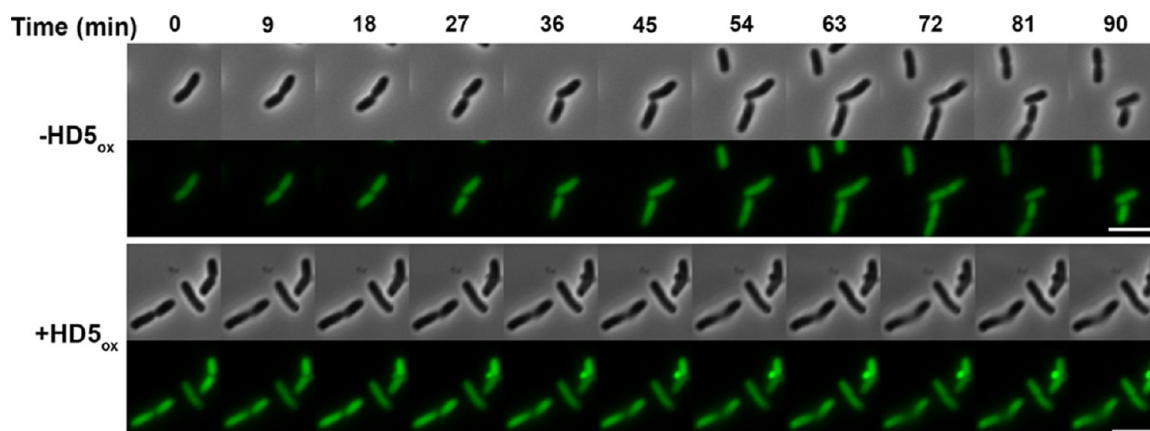


Figure 8. Time-lapse imaging of *E. coli* cyto-GFP (1×10^7 CFU/mL, mid log phase) treated with $20 \mu\text{M}$ HD5_{ox} at 37°C [10 mM sodium phosphate buffer (pH 7.4) and 1% (v/v) TSB]. The scale bar is $5 \mu\text{m}$.

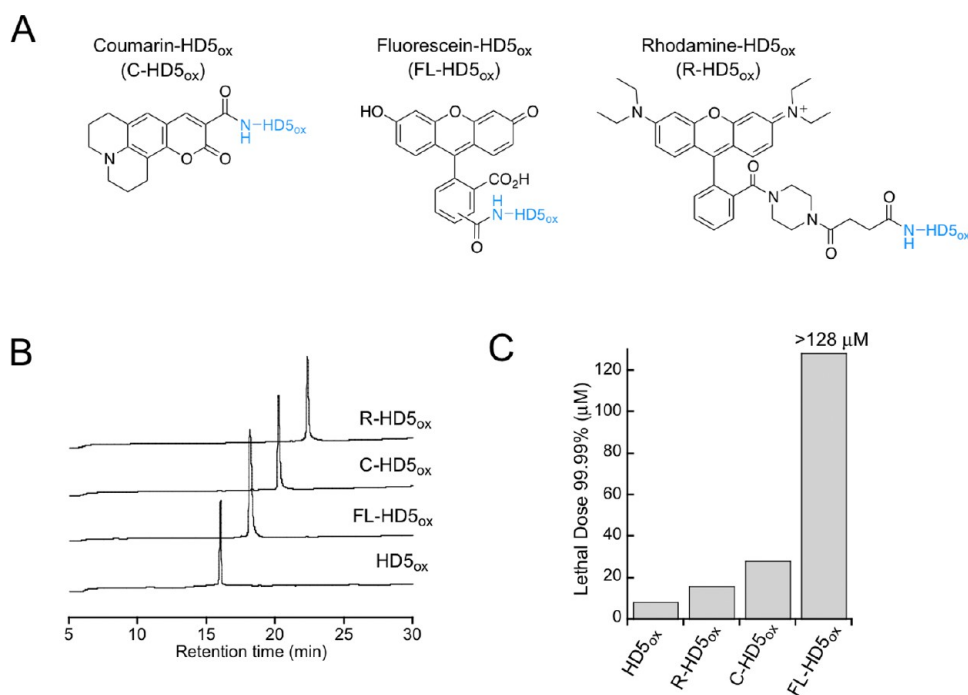


Figure 9. Functionalization of the N-terminus of HD5_{ox} affords three fluorophore–HD5_{ox} conjugates. (A) Structures of coumarin-, fluorescein-, and rhodamine-derivatized HD5_{ox}. The HD5_{ox} primary sequence is presented in Figure 1. (B) Analytical HPLC traces (220 nm absorption, 10–60% B over 30 min, 1 mL/min) of purified peptides. (C) Antimicrobial activity of the peptides against *E. coli* ATCC 25922 ($n = 3$).

(from 3.0 ± 0.8 to $2.9 \pm 0.7 \mu\text{m}$) (Student's t test, t value = 1.97, t probability = 0.049) and mean intensities (from 112 ± 38 to 139 ± 53 units) were found when stationary-phase cells were treated with HD5_{ox}.

To obtain temporal information about bleb formation and GFP redistribution, we performed time-course experiments in which *E. coli* cyto-GFP cells were treated with HD5_{ox} on the microscope stage and collected images over a 2 h period (Figure 8). The replication time for *E. coli* in the standard AMA buffer [10 mM sodium phosphate buffer (pH 7.4) and 1% (v/v) TSB without dextrose] on a MatTek plate ranged from 90 to 120 min at 37°C . These cultures were unsynchronized, and bleb formation occurred at different time points depending on the cell. Blebs were observed immediately for some cells, whereas others formed blebs after exposure to HD5_{ox} for ≈ 30 min. After the appearance of one or more blebs, the GFP intensity in the cell body diminished in all cases observed.

Although dividing *E. coli* cells were observed for untreated cells (Figure 8, top panels), cells that were affected by HD5_{ox} no longer divided (Figure 8, bottom panels).

Membrane Composition of the Blebs and Observation of Outer Membrane Vesicles. The composition of the membrane surrounding the blebs of HD5_{ox}-treated *E. coli* was investigated by fluorescence imaging of an *E. coli* strain harboring a plasmid encoding periplasmic GFP (*E. coli* peri-GFP) as well as transmission electron microscopy (TEM) of *E. coli* ATCC 25922. These studies afforded several phenotypes and suggested that two different types of blebs form (Figure S16 of the Supporting Information). Some cells exhibited a ring of GFP emission around the blebs, which indicated that both the outer and inner membranes surrounded the bleb and were intact. Other cells presented uniform GFP emission throughout the bleb. Possible explanations for this phenotype include the following: (i) only the outer membrane surrounded the blebs

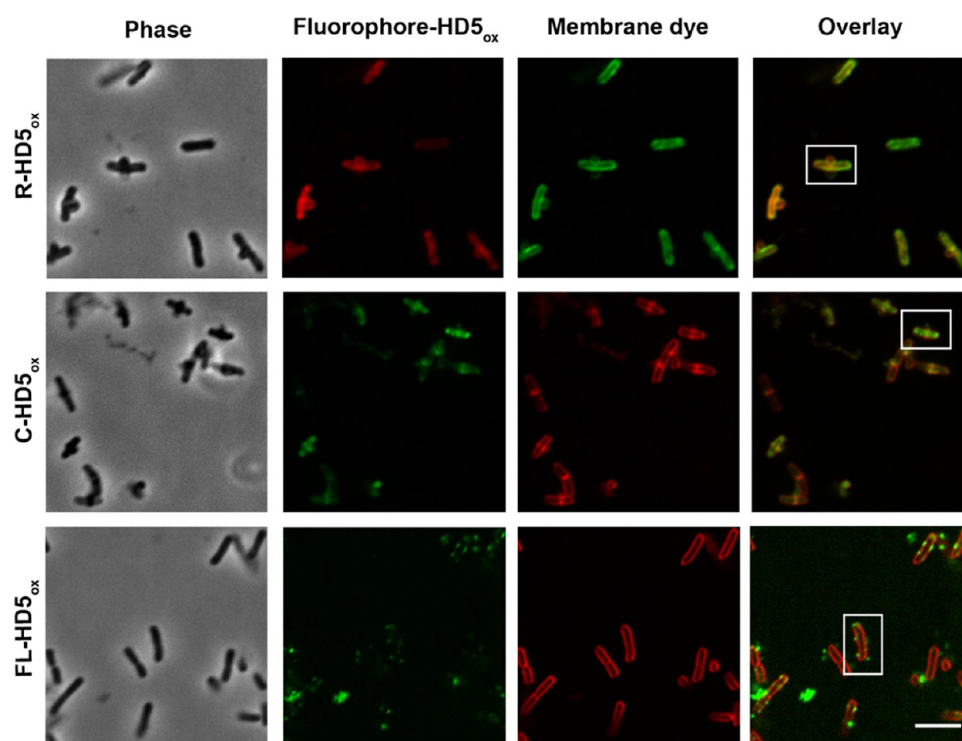


Figure 10. Fluorescence imaging of *E. coli* treated with fluorophore- HD5_{ox} conjugates and membrane dyes. *E. coli* ATCC 25922 (1×10^8 CFU/mL, mid log phase) treated with R- HD5_{ox} (20 μM), C- HD5_{ox} (20 μM), and FL- HD5_{ox} (8 μM) at 37 $^\circ\text{C}$ [10 mM sodium phosphate buffer (pH 7.4) and 1% (v/v) TSB] and incubated with 2 $\mu\text{g}/\text{mL}$ FM1-43 for the R- HD5_{ox} sample and 2 $\mu\text{g}/\text{mL}$ FM4-64 for both C- HD5_{ox} and FL- HD5_{ox} samples prior to imaging. The boxed cells are depicted in Figure 11. The scale bar is 5 μm .

or (ii) the inner membrane surrounded the bleb but was damaged and leaked the periplasmic contents into the bleb. TEM imaging revealed that the blebs are membrane-bound; however, it was difficult to confirm whether one or both membranes surround each bleb (Figure S17 of the Supporting Information).

TEM also revealed profound changes to the *E. coli* cell surface upon HD5_{ox} treatment, including vesicles surrounded by a membrane that often clustered in chainlike arrangements (Figure S17F of the Supporting Information). During phase-contrast imaging of HD5_{ox} -treated bacteria, we frequently observed surface-appended structures resembling debris. We attribute these structures, at least in part, to outer membrane vesicles (OMVs) on the basis of TEM and SEM studies (Figure S3 of the Supporting Information). Formation of OMVs (≈ 20 –200 nm wide) is an important bacterial stress response pathway, and OMVs contribute to pathogenesis.⁶³ Thus, we speculate that *E. coli* may attempt to evade HD5_{ox} by generating and shedding OMVs, along with HD5_{ox} into the extracellular space.

Design and Synthesis of Fluorophore- HD5 Conjugates for Visualizing Peptide Localization. To probe the cellular localization of HD5_{ox} , we designed, prepared, and characterized a family of fluorophore- HD5 conjugates (Figure 9A,B, Figure S18, and the Supporting Information). Because addition of a fluorophore constitutes a substantial modification to a 32-residue peptide that may perturb the function and cellular localization of the native peptide, we evaluated the behavior of fluorophore- HD5 conjugates harboring different fluorophores as well as peptides harboring rhodamine attached to different positions (Table S1 of the Supporting Information). First, we modified the N-terminus of HD5 with three

different fluorophores that afford variable photophysical properties as well as overall charge. We selected coumarin 343 (C), fluorescein (FL), and rhodamine B 4-(3-carboxypropionyl)piperazine amide (R)⁶⁴ as fluorophores to achieve emission properties spanning the range from ≈ 490 to ≈ 590 nm. Moreover, we reasoned that the overall charge of the fluorophore-modified peptide may influence its antimicrobial activity. Coumarin 343 is neutral following coupling to an α -amino group, fluorescein anionic, and rhodamine B cationic. This selection allowed us to probe the effect of fluorophore charge on the antimicrobial activity and cellular localization of fluorophore- HD5_{ox} conjugates. We prepared R- $\text{HD5}[\text{R9K}]_{\text{ox}}$ and R- $\text{HD5}[\text{R13K}]_{\text{ox}}$ to evaluate the consequences of fluorophore positioning within the peptide sequence. We selected these positions because (i) prior structure-activity relationship studies reported that R9K and R13K mutants retained some antimicrobial activity⁴⁶ and (ii) the crystal structure (PDB entry 1ZMP)²⁰ and NMR solution structure (PDB entry 2LXZ)¹⁹ of HD5_{ox} revealed that the side chains of R9 and R13 are solvent-exposed and directed away from the dimer interface of native HD5_{ox} .

The syntheses of the fluorophore- HD5 conjugates were achieved using Fmoc-based solid-phase peptide synthesis (SPPS) as described previously.⁴⁰ Analytical and photophysical characterization of the peptides is detailed in the Supporting Information (Tables S1 and S2 and Figure S18). To determine whether the absence of disulfide bonds influences cellular localization, two disulfide-null mutants, R- HD5-TE and FL- HD5-TE , were synthesized by capping the cysteines of the reduced peptides, R- HD5_{red} and FL- HD5_{red} , respectively, with 2-iodoacetamide (Supporting Information).

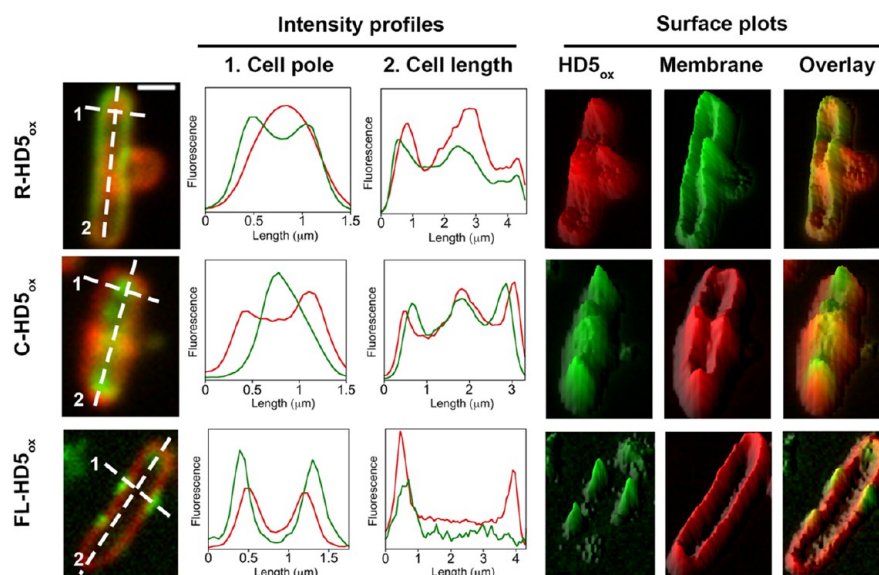


Figure 11. Intensity profiles and surface plots of the boxed cells depicted in Figure 10. Fluorescence intensities along the cell poles (dashed line 1) and across cell (dashed line 2) are plotted. Surface plots were generated using ImageJ. The scale bar is 1 μm .

Fluorophore Modifications Influence the Antibacterial Activity of HD5_{ox}. To assess the impact of fluorophore modifications on HD5_{ox} function, the AMAs of the conjugates against *E. coli* ATCC 25922 (1×10^6 CFU/mL) were first evaluated and compared to that of native HD5_{ox} (Figure 9C and Figure S18C of the Supporting Information). Fluorophore modification attenuated the cell killing ability of HD5_{ox} to varying degrees. The AMA (reported as the lethal dose for 99.99% killing, LD_{99.99}) of HD5_{ox} and the analogues harboring N-terminal fluorophores followed a trend: HD5_{ox} (8 μM) > R-HD5_{ox} (16 μM) > C-HD5_{ox} (28 μM) > FL-HD5_{ox} (>128 μM) (Figure 9C). This trend suggests that the charge of the fluorophore may influence AMA. Additional factors, such as the physiochemical properties of the fluorophores and linkers (e.g., succinic acid spacer for R-HD5_{ox}), may also contribute to such changes in the AMA of modified HD5_{ox}. R-HD5[R13K]_{ox} and R-HD5[R13K]_{ox} were active against *E. coli*, and the linear derivatives were less active than their respective folded peptides, as expected (Figure S18C of the Supporting Information).

HD5_{ox} Enters the *E. coli* Cytoplasm and Localizes at the Cell Poles and Division Site. On the basis of the AMA assay results described above, we first investigated the cellular localization of R-HD5_{ox}. We observed HD5_{ox}-like morphological changes, including bleb formation, for *E. coli* ATCC 25922 (Figure 10) and *E. coli* CFT073 (Figure S19 of the Supporting Information). Intracellular fluorescence was also observed. Co-labeling studies with the membrane-binding dye FM1-43 revealed that the FM1-43 emission profile enclosed a significant portion of the R-HD5_{ox} fluorescence intensity profile (Figures 10 and 11), which indicates that the peptide penetrated the outer and inner membranes and entered the cytoplasm. In most of the cells examined by fluorescence microscopy, the rhodamine emission was most intense at the poles and division plane. This type of labeling pattern was not observed for R-HD5-TE or rhodamine-modified LL-37 (Figure S20 of the Supporting Information), both of which provided uniform cytoplasmic fluorescence.

When *E. coli* cells were treated with R-HD5_{ox} under conditions that result in attenuated HD5_{ox} activity (*vide supra*),

different labeling patterns were observed. For instance, the presence of NaCl (200 mM) resulted in rhodamine emission only at the cell surface, indicating that R-HD5_{ox} did not enter *E. coli* (Figure S22 of the Supporting Information). Stationary-phase *E. coli* treated with R-HD5_{ox} exhibited diminished intracellular fluorescence relative to that of mid log-phase cells (Figure S22 of the Supporting Information). Taken together, these observations support a model whereby HD5_{ox} must overcome the outer membrane permeability barrier and enter the cytosol to exert its full capacity to kill bacteria.

Co-incubation of *E. coli* with a 1:1 molar ratio of rhodamine B and HD5_{ox} resulted in uniform cytoplasmic staining, whereas treatment of *E. coli* with rhodamine B alone resulted in negligible cellular fluorescence (Figure S21 of the Supporting Information). This result suggested that HD5_{ox} treatment allowed for rhodamine B entry as a result of membrane permeabilization and confirmed that covalent attachment of rhodamine to HD5_{ox} is essential for observing fluorescence localized to the cell poles and division site. The R-HD5[R13K]_{ox} conjugate provided a labeling pattern similar to that of R-HD5_{ox} and thereby indicated that localization of the R-HD5_{ox} conjugate is not an artifact resulting from a particular site of rhodamine attachment (Figure S20 of the Supporting Information). Moreover, C-HD5_{ox} preferentially labeled the cell poles and cell division sites, and co-labeling with the membrane-binding dye FM4-64 confirmed its cytoplasmic localization (Figures 10 and 11). The fact that the same labeling pattern was observed for HD5_{ox} modified with either rhodamine or coumarin, taken with these modified peptides causing the same morphological changes as observed for unmodified HD5_{ox}, provides a strong indication that the localization is a result of HD5_{ox} and not the fluorophore.

It should be noted that FL-HD5_{ox}, which provided no *in vitro* antibacterial activity against *E. coli* at the highest concentration evaluated (128 μM), did not enter *E. coli*. Rather, the peptide afforded a punctate labeling pattern on and around the bacterial surface (Figures 10 and 11). We attribute this phenomenon to the overall negative charge of the fluorescein moiety.

The fluorescence imaging studies of HD5_{ox} may be considered in the context of other AMPs that have been examined by similar approaches to probe uptake and mechanism of action. For instance, fluorescence microscopy revealed that buforin II entered the bacterial cytoplasm without permeabilizing the inner membrane.⁶⁵ A rhodamine derivative of the only human cathelicidin, LL-37, attacked septating *E. coli* more readily than nonseptating cells and permeabilized the bacteria via a carpet model of membrane destabilization.^{66,67} A fluorophore-labeled lantibiotic was shown to interact with lipid II of *Bacillus subtilis* 168.⁶⁸ Recent imaging studies of Cy3-derivatized HBD2 indicated that HBD2 preferentially localizes to the nascent poles and cell division site of *E. faecalis*.³¹ This focal labeling pattern was attributed to the binding of the HBD2 to anionic lipids in these regions. The cell poles and division site of *E. coli* are also enriched in negatively charged phospholipids that include cardiolipin and phosphatidylglycerol.⁶⁹ Whether HD5_{ox} also binds to anionic lipids at the cell poles of *E. coli* and/or another target in these locales is currently unknown and a topic for future investigation.

SUMMARY AND OUTLOOK

In this study, we defined how the antimicrobial peptide HD5_{ox} affects the morphology of *E. coli* and other Gram-negative bacteria. We established that HD5_{ox} causes distinct morphological changes to *E. coli* as well as *K. pneumoniae*, *A. baumannii*, and *P. aeruginosa* that include bleb formation, cellular clumping, and elongation. We also demonstrated that other AMPs, including human LL-37 and murine α -defensin cryptdin-4, do not cause such morphologies. Taken together, these observations indicate that HD5_{ox} kills *E. coli* by a mechanism different from those of the other peptides examined in this work. Our results highlight the importance of treating host-defense peptides individually and not generalizing cell killing mechanisms.

Defensins are often described as membrane-disrupting peptides. Our prior investigations indicate that HD5_{ox} traverses the outer membrane and subsequently damages the inner membrane of *E. coli*.^{44,50} In this work, the insights gained from utilizing fluorophore-HD5_{ox} conjugates modified with rhodamine or coumarin support a model in which HD5_{ox} enters the *E. coli* cytoplasm. Because the cytoplasm is a reducing environment, intracellular reduction of the HD5_{ox} disulfide array to liberate free cysteine residues may occur. Deciphering whether such redox chemistry contributes to altered cellular morphologies and cell killing warrants exploration. The cytoplasmic localization also supports the possibility that HD5_{ox} (or the reduced form) has an as yet undiscovered intracellular target. Indeed, the intracellular staining pattern at the cell poles and cell division site routinely observed for *E. coli* treated with R- and/or C-HD5_{ox} suggest the locale of a possible target. On the basis of this localization, coupled with the elongation phenotype observed for *E. coli* and other Gram-negative microbes, we reason that HD5_{ox} may exert antimicrobial activity by affecting cell division. Efforts are underway to further investigate this notion.

ASSOCIATED CONTENT

Supporting Information

Complete experimental methods and additional data. This material is available free of charge via the Internet at <http://pubs.acs.org>.

AUTHOR INFORMATION

Corresponding Author

*E-mail: Inolan@mit.edu. Phone: (617) 452-2495. Fax: (617) 324-0505.

Funding

This work was supported by the National Institutes of Health (Grant DP2OD007045 from the Office of the Director). H.R.C. was a recipient of a 2014 Richard R. Schrock summer graduate fellowship. P.C. is a recipient of a Royal Thai Government Fellowship. S.A.L. and I-L.C. received research funding from the Massachusetts Institute of Technology UROP Program. The Biophysical Instrumentation Facility for the Study of Complex Macromolecular Systems (National Science Foundation Grant 007031) is gratefully acknowledged. The Institute for Soldier Nanotechnologies is supported in part by the U.S. Army Research Laboratory and the U.S. Army Research Office through the Institute for Soldier Nanotechnologies, under Contract W911NF-13-D-0001.

Notes

The authors declare no competing financial interest.

ACKNOWLEDGMENTS

We thank Prof. D. Kahne for insightful discussions, Prof. B. L. Pentelute and members of the Pentelute laboratory for expertise in flow-based peptide synthesis, Yunfei Zhang for performing initial Zn(II) experiments, Jill Tomaras for microbiology assistance, Nicki Watson of the Whitehead Institute for Biomedical Research for preparing the TEM samples and imaging, Prof. K. Ribbeck for providing the *E. coli* cyto-GFP strain, and Prof. K. D. Young for providing pDKR2(dsba_{ss}-sfgfp) that was employed to make *E. coli* per-GFP.

ABBREVIATIONS

AMA, antimicrobial activity; C, coumarin 343; CFU, colony-forming unit; CFU/mL, colony-forming units per milliliter; Crp-4, cryptdin-4 (a murine α -defensin); FL, 5(6)-carboxy-fluorescein; FM1-43, N-(3-triethylammoniumpropyl)-4-[4-(dibutylamino)styryl]pyridinium dibromide; FM4-64, N-(3-triethylammoniumpropyl)-4-[6-[4-(diethylamino)phenyl]-hexatrienyl]pyridinium dibromide; HD5, human α -defensin 5; HD5_{red}, reduced form of human α -defensin 5; HD5_{ox}, oxidized form of human α -defensin 5; HD5-TE, linear form of human α -defensin 5 (iodoacetamide-capped); HD5-CD, human α -defensin 5 covalent dimer; NMR, nuclear magnetic resonance; PDB, Protein Data Bank; PI, propidium iodide; R, rhodamine B 4-(3-carboxypropionyl)piperazine amide; SEM, scanning electron microscopy; TEM, transmission electron microscopy; TSB, trypticase soy broth.

REFERENCES

- (1) World Health Organization (2014) Antimicrobial resistance: Global report on surveillance, World Health Organization, Geneva.
- (2) Davies, J., and Davies, D. (2010) Origins and evolution of antibiotic resistance. *Microbiol. Mol. Biol. Rev.* 74, 417–433.
- (3) Fischbach, M. A., and Walsh, C. T. (2009) Antibiotics for emerging pathogens. *Science* 325, 1089–1093.
- (4) Lewis, K. (2013) Platforms for antibiotic discovery. *Nat. Rev. Drug Discovery* 12, 371–387.
- (5) Jenssen, H., Hamill, P., and Hancock, R. E. W. (2006) Peptide antimicrobial agents. *Clin. Microbiol. Rev.* 19, 491–511.

- (6) Choi, K.-Y., Chow, L. N. Y., and Mookherjee, N. (2012) Cationic host defence peptides: Multifaceted role in immune modulation and inflammation. *J. Innate Immun.* 4, 361–370.
- (7) Lehrer, R. I., and Lu, W. (2012) α -Defensins in human innate immunity. *Immunol. Rev.* 245, 84–112.
- (8) Cruz, J., Ortiz, C., Guzmán, F., Fernández-Lafuente, R., and Torres, R. (2014) Antimicrobial peptides: Promising compounds against pathogenic microorganisms. *Curr. Med. Chem.* 21, 2299–2321.
- (9) Ganz, T. (2003) Defensins: Antimicrobial peptides of innate immunity. *Nat. Rev. Immunol.* 3, 710–720.
- (10) Ramanathan, B., Davis, E. G., Ross, C. R., and Blecha, F. (2002) Cathelicidins: Microbicidal activity, mechanisms of action, and roles in innate immunity. *Microbes Infect.* 4, 361–372.
- (11) Gennaro, R., and Zanetti, M. (2000) Structural features and biological activities of the cathelicidin-derived antimicrobial peptides. *Biopolymers* 55, 31–49.
- (12) Selsted, M. E., and Ouellette, A. J. (2005) Mammalian defensins in the antimicrobial immune response. *Nat. Immunol.* 6, 551–557.
- (13) Jones, D. E., and Bevins, C. L. (1992) Paneth cells of the human small intestine express an antimicrobial peptide gene. *J. Biol. Chem.* 267, 23216–23225.
- (14) Porter, E. M., Liu, L., Oren, A., Anton, P. A., and Ganz, T. (1997) Localization of human intestinal defensin 5 in Paneth cell granules. *Infect. Immun.* 65, 2389–2395.
- (15) Ayabe, T., Ashida, T., Kohgo, Y., and Kono, T. (2004) The role of Paneth cells and their antimicrobial peptides in innate host defense. *Trends Microbiol.* 12, 394–398.
- (16) Clevers, H. C., and Bevins, C. L. (2013) Paneth cells: Maestros of the small intestinal crypts. *Annu. Rev. Physiol.* 75, 289–311.
- (17) Brogden, K. A. (2005) Antimicrobial peptides: Pore formers or metabolic inhibitors in bacteria? *Nat. Rev. Microbiol.* 3, 238–250.
- (18) Hilchie, A. L., Wuerth, K., and Hancock, R. E. W. (2013) Immune modulation by multifaceted cationic host defense (antimicrobial) peptides. *Nat. Chem. Biol.* 9, 761–768.
- (19) Wommack, A. J., Robson, S. A., Wanniarachchi, Y. A., Wan, A., Turner, C. J., Wagner, G., and Nolan, E. M. (2012) NMR solution structure and condition-dependent oligomerization of the antimicrobial peptide human defensin 5. *Biochemistry* 51, 9624–9637.
- (20) Szyk, A., Wu, Z., Tucker, K., Yang, D., Lu, W., and Lubkowsky, J. (2006) Crystal structures of human α -defensins HNP4, HDS, and HD6. *Protein Sci.* 15, 2749–2760.
- (21) Lehrer, R. I., Barton, A., Daher, K. A., Harwig, S. S., Ganz, T., and Selsted, M. E. (1989) Interaction of human defensins with *Escherichia coli*. Mechanism of bactericidal activity. *J. Clin. Invest.* 84, 553–561.
- (22) Zasloff, M. (2002) Antimicrobial peptides of multicellular organisms. *Nature* 415, 389–395.
- (23) Figueredo, S. M., Weeks, C. S., Young, S. K., and Ouellette, A. J. (2009) Anionic amino acids near the pro- α -defensin N terminus mediate inhibition of bactericidal activity in mouse pro-cryptdin-4. *J. Biol. Chem.* 284, 6826–6831.
- (24) Hill, C. P., Yee, J., Selsted, M. E., and Eisenberg, D. (1991) Crystal structure of defensin HNP-3, an amphiphilic dimer: Mechanisms of membrane permeabilization. *Science* 251, 1481–1485.
- (25) Schneider, T., Kruse, T., Wimmer, R., Wiedemann, I., Sass, V., Pag, U., Jansen, A., Nielsen, A. K., Mygind, P. H., Raventós, D. S., Neve, S., Ravn, B., Bonvin, A. M. J. J., De Maria, L., Andersen, A. S., Gammelgaard, L. K., Sahl, H.-G., and Kristensen, H.-H. (2010) Plectasin, a fungal defensin, targets the bacterial cell wall precursor Lipid II. *Science* 328, 1168–1172.
- (26) Schmitt, P., Wilmes, M., Pugnère, M., Aumelas, A., Bachère, E., Sahl, H.-G., Schneider, T., and Destoumieux-Garzon, D. (2010) Insight into invertebrate defensin mechanism of action: Oyster defensins inhibit peptidoglycan biosynthesis by binding to lipid II. *J. Biol. Chem.* 285, 29208–29216.
- (27) Essig, A., Hofmann, D., Münch, D., Gayathri, S., Künzler, M., Kallio, P. T., Sahl, H.-G., Wider, G., Schneider, T., and Aebi, M. (2014) Copsin, a novel peptide-based fungal antibiotic interfering with the peptidoglycan synthesis. *J. Biol. Chem.* 289, 34953–34964.
- (28) de Leeuw, E., Li, C., Zeng, P., Li, C., Diepeveen-de Buin, M., Lu, W.-Y., Breukink, E., and Lu, W. (2010) Functional interaction of human neutrophil peptide-1 with the cell wall precursor lipid II. *FEBS Lett.* 584, 1543–1548.
- (29) Sass, V., Schneider, T., Wilmes, M., Körner, C., Tossi, A., Novikova, N., Shamova, O., and Sahl, H.-G. (2010) Human β -defensin 3 inhibits cell wall biosynthesis in *Staphylococci*. *Infect. Immun.* 78, 2793–2800.
- (30) Wilmes, M., and Sahl, H.-G. (2014) Defensin-based anti-infective strategies. *Int. J. Med. Microbiol.* 304, 93–99.
- (31) Kandaswamy, K., Liew, T. H., Wang, C. Y., Huston-Warren, E., Meyer-Hoffert, U., Hultén, K., Schröder, J. M., Caparon, M. G., Normark, S., Henriques-Normark, B., Hultgren, S. J., and Kline, K. A. (2013) Focal targeting by human β -defensin 2 disrupts localized virulence factor assembly sites in *Enterococcus faecalis*. *Proc. Natl. Acad. Sci. U.S.A.* 110, 20230–20235.
- (32) Chu, H., Pazgier, M., Jung, G., Nuccio, S.-P., Castillo, P. A., de Jong, M. F., Winter, M. G., Winter, S. E., Wehkamp, J., Shen, B., Salzman, N. H., Underwood, M. A., Tsolis, R. M., Young, G. M., Lu, W., Lehrer, R. I., Bäuml, A. J., and Bevins, C. L. (2012) Human α -defensin 6 promotes mucosal innate immunity through self-assembled peptide nanonets. *Science* 337, 477–481.
- (33) Chairatana, P., and Nolan, E. M. (2014) Molecular basis for self-assembly of a human host-defense peptide that entraps bacterial pathogens. *J. Am. Chem. Soc.* 136, 13267–13276.
- (34) Giblin, L. J., Chang, C. J., Bentley, A. F., Frederickson, C., Lippard, S. J., and Frederickson, C. J. (2006) Zinc-secreting Paneth cells studied by ZP fluorescence. *J. Histochem. Cytochem.* 54, 311–316.
- (35) Dinsdale, D. (1984) Ultrastructural localization of zinc and calcium within the granules of rat Paneth cells. *J. Histochem. Cytochem.* 32, 139–145.
- (36) Wehkamp, J., Salzman, N. H., Porter, E., Nuding, S., Weichenthal, M., Petras, R. E., Shen, B., Schaeffeler, E., Schwab, M., Linzmeier, R., Feathers, R. W., Chu, H., Lima, H., Fellermann, K., Ganz, T., Stange, E. F., and Bevins, C. L. (2005) Reduced Paneth cell α -defensins in ileal Crohn's disease. *Proc. Natl. Acad. Sci. U.S.A.* 102, 18129–18134.
- (37) Ericksen, B., Wu, Z., Lu, W., and Lehrer, R. I. (2005) Antibacterial activity and specificity of the six human α -defensins. *Antimicrob. Agents Chemother.* 49, 269–275.
- (38) Porter, E. M., van Dam, E., Valore, E. V., and Ganz, T. (1997) Broad-spectrum antimicrobial activity of human intestinal defensin 5. *Infect. Immun.* 65, 2396–2401.
- (39) Nuding, S., Zabel, L. T., Enders, C., Porter, E., Fellermann, K., Wehkamp, J., Mueller, H. A. G., and Stange, E. F. (2009) Antibacterial activity of human defensins on anaerobic intestinal bacterial species: A major role of HBD-3. *Microbes Infect.* 11, 384–393.
- (40) Wommack, A. J., Ziarek, J. J., Tomaras, J., Chileveru, H. R., Zhang, Y., Wagner, G., and Nolan, E. M. (2014) Discovery and characterization of a disulfide-locked C₂-symmetric defensin peptide. *J. Am. Chem. Soc.* 136, 13494–13497.
- (41) Salzman, N. H., Ghosh, D., Huttner, K. M., Paterson, Y., and Bevins, C. L. (2003) Protection against enteric salmonellosis in transgenic mice expressing a human intestinal defensin. *Nature* 422, 522–526.
- (42) Salzman, N. H., Hung, K., Haribhai, D., Chu, H., Karlsson-Sjöberg, J., Amir, E., Tegatz, P., Barman, M., Hayward, M., Eastwood, D., Stoel, M., Zhou, Y., Sodergren, E., Weinstock, G. M., Bevins, C. L., Williams, C. B., and Bos, N. A. (2010) Enteric defensins are essential regulators of intestinal microbial ecology. *Nat. Immunol.* 11, 76–83.
- (43) Rajabi, M., Ericksen, B., Wu, X., de Leeuw, E., Zhao, L., Pazgier, M., and Lu, W. (2012) Functional determinants of human enteric α -defensin HDS: Crucial role for hydrophobicity at dimer interface. *J. Biol. Chem.* 287, 21615–21627.
- (44) Wanniarachchi, Y. A., Kaczmarek, P., Wan, A., and Nolan, E. M. (2011) Human defensin 5 disulfide array mutants: Disulfide bond deletion attenuates antibacterial activity against *Staphylococcus aureus*. *Biochemistry* 50, 8005–8017.

- (45) De Leeuw, E., Burks, S. R., Li, X., Kao, J. P. Y., and Lu, W. (2007) Structure-dependent functional properties of human defensin 5. *FEBS Lett.* 581, 515–520.
- (46) De Leeuw, E., Rajabi, M., Zou, G., Pazgier, M., and Lu, W. (2009) Selective arginines are important for the antibacterial activity and host cell interaction of human α -defensin 5. *FEBS Lett.* 583, 2507–2512.
- (47) Rajabi, M., de Leeuw, E., Pazgier, M., Li, J., Lubkowski, J., and Lu, W. (2008) The conserved salt bridge in human α -defensin 5 is required for its precursor processing and proteolytic stability. *J. Biol. Chem.* 283, 21509–21518.
- (48) Wei, G., de Leeuw, E., Pazgier, M., Yuan, W., Zou, G., Wang, J., Ericksen, B., Lu, W.-Y., Lehrer, R. I., and Lu, W. (2009) Through the looking glass, mechanistic insights from enantiomeric human defensins. *J. Biol. Chem.* 284, 29180–29192.
- (49) Thomassin, J.-L., Lee, M. J., Brannon, J. R., Sheppard, D. C., Gruenheid, S., and Le Moual, H. (2013) Both group 4 capsule and lipopolysaccharide O-antigen contribute to enteropathogenic *Escherichia coli* resistance to human α -defensin 5. *PLoS One* 8, e82475.
- (50) Moser, S., Chileveru, H. R., Tomaras, J., and Nolan, E. M. (2014) A bacterial mutant library as a tool to study the attack of a defense peptide. *ChemBioChem* 15, 2684–2688.
- (51) Schmidt, N. W., Mishra, A., Lai, G. H., Davis, M., Sanders, L. K., Tran, D., Garcia, A., Tai, K. P., McCray, P. B., Jr., Ouellette, A. J., Selsted, M. E., and Wong, G. C. L. (2011) Criterion for amino acid composition of defensins and antimicrobial peptides based on geometry of membrane destabilization. *J. Am. Chem. Soc.* 133, 6720–6727.
- (52) van den Bogaart, G., Guzmán, J. V., Mika, J. T., and Poolman, B. (2008) On the mechanism of pore formation by melittin. *J. Biol. Chem.* 283, 33854–33857.
- (53) Falagas, M. E., and Kasiakou, S. K. (2005) Colistin: The revival of polymyxins for the management of multidrug-resistant Gram-negative bacterial infections. *Clin. Infect. Dis.* 40, 1333–1341.
- (54) Sochacki, K. A., Barns, K. J., Bucki, R., and Weisshaar, J. C. (2011) Real-time attack on single *Escherichia coli* cells by the human antimicrobial peptide LL-37. *Proc. Natl. Acad. Sci. U.S.A.* 108, E77–E81.
- (55) Matsuzaki, K., Sugishita, K., Harada, M., Fujii, N., and Miyajima, K. (1997) Interactions of an antimicrobial peptide, magainin 2, with outer and inner membranes of Gram-negative bacteria. *Biochim. Biophys. Acta* 1327, 119–130.
- (56) Spindler, E. C., Hale, J. D. F., Giddings, T. H., Jr., Hancock, R. E. W., and Gill, R. T. (2011) Deciphering the mode of action of the synthetic antimicrobial peptide Bac8c. *Antimicrob. Agents Chemother.* 55, 1706–1716.
- (57) Yao, Z., Kahne, D., and Kishony, R. (2012) Distinct single-cell morphological dynamics under β -lactam antibiotics. *Mol. Cell* 48, 705–712.
- (58) Paradis-Bleau, C., Kritikos, G., Orlova, K., Typas, A., and Bernhardt, T. G. (2014) A genome-wide screen for bacterial envelope biogenesis mutants identifies a novel factor involved in cell wall precursor metabolism. *PLoS Genet.* 10, e1004056.
- (59) Yeh, Y.-C., Comolli, L. R., Downing, K. H., Shapiro, L., and McAdams, H. H. (2010) The caulobacter Tol-Pal complex is essential for outer membrane integrity and the positioning of a polar localization factor. *J. Bacteriol.* 192, 4847–4858.
- (60) Goldman, M. J., Anderson, G. M., Stolzenberg, E. D., Kari, U. P., Zasloff, M., and Wilson, J. M. (1997) Human β -defensin-1 is a salt-sensitive antibiotic in lung that is inactivated in cystic fibrosis. *Cell* 88, 553–560.
- (61) Zhang, Y., Cougnon, F. B. L., Wanniarachchi, Y. A., Hayden, J. A., and Nolan, E. M. (2013) Reduction of human defensin 5 affords a high-affinity zinc-chelating peptide. *ACS Chem. Biol.* 8, 1907–1911.
- (62) Chung, H. S., Yao, Z., Goehring, N. W., Kishony, R., Beckwith, J., and Kahne, D. (2009) Rapid β -lactam-induced lysis requires successful assembly of the cell division machinery. *Proc. Natl. Acad. Sci. U.S.A.* 106, 21872–21877.
- (63) Kulp, A., and Kuehn, M. J. (2010) Biological functions and biogenesis of secreted bacterial outer membrane vesicles. *Annu. Rev. Microbiol.* 64, 163–184.
- (64) Nguyen, T., and Francis, M. B. (2003) Practical synthetic route to functionalized rhodamine dyes. *Org. Lett.* 5, 3245–3248.
- (65) Park, C. B., Yi, K.-S., Matsuzaki, K., Kim, M. S., and Kim, S. C. (2000) Structure-activity analysis of buforin II, a histone H2A-derived antimicrobial peptide: The proline hinge is responsible for the cell-penetrating ability of buforin II. *Proc. Natl. Acad. Sci. U.S.A.* 97, 8245–8250.
- (66) Barns, K. J., and Weisshaar, J. C. (2013) Real-time attack of LL-37 on single *Bacillus subtilis* cells. *Biochim. Biophys. Acta* 1828, 1511–1520.
- (67) Ding, B., Soblosky, L., Nguyen, K., Geng, J., Yu, X., Ramamoorthy, A., and Chen, Z. (2013) Physiologically-relevant modes of membrane interactions by the human antimicrobial peptide, LL-37, revealed by SFG experiments. *Sci. Rep.* 3, 1854.
- (68) Bindman, N. A., and van der Donk, W. A. (2013) A general method for fluorescent labeling of the N-termini of lanthipeptides and its application to visualize their cellular localization. *J. Am. Chem. Soc.* 135, 10362–10371.
- (69) Oliver, P. M., Crooks, J. A., Leidl, M., Yoon, E. J., Saghatelian, A., and Weibel, D. B. (2014) Localization of Anionic Phospholipids in *Escherichia coli* Cells. *J. Bacteriol.* 196, 3386–3398.